Detection of feline coronavirus using microcantilever sensors

2006 Meas. Sci. Technol. 17 2964

(http://iopscience.iop.org/0957-0233/17/11/015)

INSTITUTE OF PHYSICS PUBLISHING MEASUREMENT SCIENCE AND TECHNOLOGY

Meas. Sci. Technol. **17** (2006) 2964–2968 doi:10.1088/0957-0233/17/11/015

Detection of feline coronavirus using microcantilever sensors

Sreepriya Velanki and Hai-Feng Ji[1]

Chemistry Program and Institute for Micromanufacturing, Louisiana Tech University, Ruston, LA 71270, USA

E-mail: hji@chem.latech.edu

Received 23 May 2006, in final form 7 August 2006
Published 5 October 2006
Online at stacks.iop.org/MST/17/2964

Abstract

This work demonstrated the feasibility of detecting severe acute respiratory syndrome associated coronavirus (SARS-CoV) using microcantilever technology by showing that the feline coronavirus (FIP) type I virus can be detected by a microcantilever modified by feline coronavirus (FIP) type I anti-viral antiserum. A microcantilever modified by FIP type I anti-viral antiserum was developed for the detection of FIP type I virus. When the FIP type I virus positive sample is injected into the fluid cell where the microcantilever is held, the microcantilever bends upon the recognition of the FIP type I virus by the antiserum on the surface of the microcantilever. A negative control sample that does not contain FIP type I virus did not cause any bending of the microcantilever. The detection limit of the sensor was 0.1 μg ml^{-1} when the assay time was $<$1 h.

Keywords: microcantilever, feline coronavirus (FIP) detection, SARS detection, adsorption-induced surface stress

Introduction

Severe acute respiratory syndrome (SARS), a viral respiratory disease, first emerged in the Guangdong province in China during November 2002 [1, 2]. Within a span of a few months, the disease spread rapidly in Southeast Asia and other parts of the world. The epidemic spanned almost 30 countries and created a global alert [1, 3]. SARS is characterized by high fever, malaise, rigor, headache and dyspnoea and may progress to generalized interstitial infiltrates in the lungs requiring artificial ventilation. The fatality rate may be as high as 15% [4, 5]. SARS is believed to have originated from healthy Himalayan palm civets (*Paguma larvata*), a cat-like mammal closely related to the mongoose. The causative organism for this disease was a coronavirus, called the SARS associated coronavirus (SARS-CoV). Coronaviruses (order Nidovirales, family Coronaviridae, genus Coronavirus) belong to a family of large, enveloped, positive sense, single stranded RNA viruses that replicate in the cytoplasm of animal host cells. The genomes of the coronavirus are the largest of the RNA viruses ranging from 27 kb to 32 kb in length. The virus varies from 100–140 nm in diameter. The viral particles have characteristic surface projections called peplomers, which are about 20 nm long and 10 nm wide. This crown-like appearance (Latin—*Corona*) gives the virus family its name [5].

Severe acute respiratory syndrome has relatively high transmissibility and mortality upon infection [6]. Hence, diagnostic tests have since then evinced a keen interest amongst researchers all over the world [1–11].

Since the early nineties of the last century, microcantilevers have been emerging as novel platforms for sensors with on-chip circuitry and extremely good sensitivity [11–16]. Selectivity of the microcantilevers can be achieved by modifying the surface of the microcantilevers by coatings or by covalently binding molecular recognition agents for identification of chemically or biologically specific species. Microcantilevers possess the unique characteristic of bending under the influence of differential stresses produced when the molecular adsorption is confined to one side of the cantilever [12–16]. Microcantilever sensors bend in both air and solution. Four methods may be used for cantilever detection, namely optical [17], piezoresistive [18], piezoelectric [19] and capacitive [20].

[1] Corresponding author: Hai-Feng (Frank) Ji, PhD, Associate Professor of Chemistry, Louisiana Tech University, 911 Hergot Ave., Ruston, LA 71272, USA.

Microcantilever sensors have already made their foray into the detection of biological species such as bacteria, viruses, etc [21]. Since SARS-CoV is very contagious and handling it is severely restricted by governmental regulations, this work presents a microcantilever based sensor for the detection of feline coronavirus (FIP), a virus whose structure is similar to SARS-CoV. Feline coronavirus is known to be highly prevalent in the cat population, affecting both domestic cats and also those in catteries [22, 23]. It causes a deadly disease called feline infectious peritonitis (FIP) amongst cats. We wish to demonstrate the feasibility of detecting SARS-CoV using microcantilever technology by showing that FIP can be detected by a microcantilever modified by feline coronavirus (FIP) type I anti-viral antiserum.

Experimental section

Microcantilevers

In our experiments, we used commercially available silicon microcantilevers (Veeco Instruments). The dimensions of the V-shaped silicon microcantilevers were 180 μm in length, 25 μm in leg width and 1 μm in thickness. One side of these cantilevers was covered with a thin film of chromium (3 nm), followed by a 20 nm layer of gold, both deposited by e-beam evaporation. On the uncoated side of the commercial microcantilever was silicon with a naturally grown 12–19 Å thick SiO_2 layer called 'native oxide'.

The shape of the MCL used in this work is shown in scheme 1.

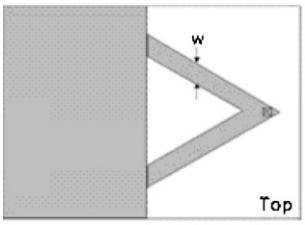

Scheme 1. Top view of the MCL (Veeco Instruments, Santa Barbara, CA) used in these experiments.

Reagents and materials

11-Mercaptoundecanoic acid, absolute ethyl alcohol, coupling agents, such as 1-ethyl-3-(3-dimethylaminopropyl) carbodiimide hydrochloride (EDC) and N-hydroxysulfo-succinimide (NHS), were purchased from Sigma Aldrich. The polyclonal antibody immobilized on the microcantilever was type I feline coronavirus (FIP) anti-viral antiserum, and the inactivated antigen was feline infectious peritonitis virus type I (FIP I). Both the antigen and antibody were purchased from VMRD, Inc.

Antibody immobilization

Two protocols have been used for antibody immobilization:

Protocol 1. Surface modification was accomplished according to a known surface conjugation technique [24]. A thin film of aminopropyltriethoxysilane (ATS) was formed on the silicon side of the microcantilever by immersing the cantilevers in a 1% ATS solution of 95 : 5 = ethanol:water for a period of 24 h at room temperature. This was followed by the rinsing of the microcantilever in DI water. The cantilevers were then immersed in 10% succinic anhydride solution in N_2 saturated N,N-dimethylformamide (DMF) for 6 h, followed by a thorough rinsing step of the microcantilevers in DI water. Next, the cantilevers were dipped in 0.05 mM of 4-morpholinepropanesulfonic acid (MES) buffer solution containing 100 mg ml^{-1} of EDC and 100 mg ml^{-1} of NHS (pH = 6.8) for 30 min at room temperature followed by DI water rinsing. The last step was the immobilization of the antibody on the microcantilever. This was done by incubating the modified microcantilevers in 1 ml of phosphate buffer solution containing 2 μl of antibody (feline infectious peritonitis virus type I polyclonal anti-viral antiserum) at room temperature for 3 h.

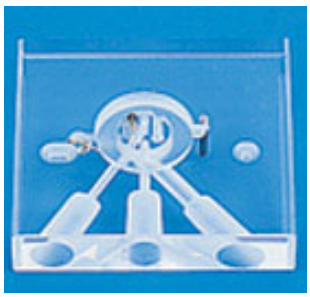

Figure 1. Fluid cell used in these experiments.
(This figure is in colour only in the electronic version)

Protocol 2. Clean microcantilevers were stored overnight in a 1 mM ethanolic solution of 11-mercaptoundecanoic acid. Then, these microcantilevers were thoroughly rinsed with distilled water before being immersed in a solution of 0.5 M NHS and 0.2 M EDC in distilled water for a time period of 30–45 min [25]. This was followed by thorough rinsing of the cantilevers in DI water to remove excess chemicals. The final step was the immobilization of the antibody on the microcantilever. 5 μl of the FIP anti-viral antiserum was dissolved in 1 ml of phosphate buffer solution. The microcantilevers were incubated in this solution for a period of 3 h. The microcantilevers were then rinsed to remove any excess antibody. The chemically modified microcantilevers were stored in buffer solution before use.

Equipment and apparatus

The deflection experiments are performed in a flow-through glass cell (figure 1, Digital Instruments, Santa Barbara, CA) such as those used in AFM. Microcantilever deflection measurements based on the optical beam deflection method were carried out using a photodiode. The deflection of the cantilever was measured by monitoring the position of a laser beam reflected from the cantilever onto a four-quadrant photodiode. A syringe pump was used to inject the working solution while the analyte of interest is injected using a low pressure injection port sample loop system. A schematic diagram of the apparatus used in this study was previously reported [26].

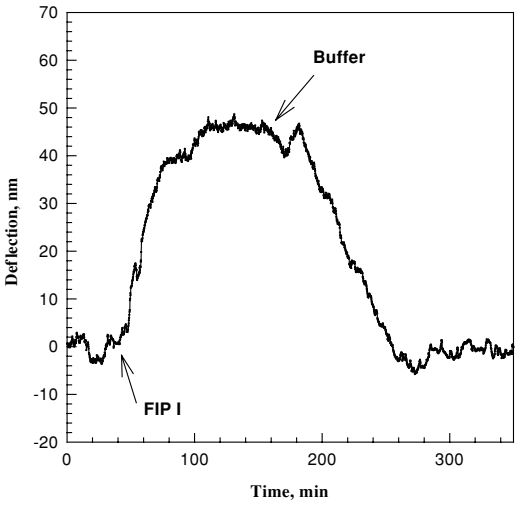

Figure 2. Deflection of a FIP antiserum modified microcantilever versus time after injection of a 3.9 μg ml^{-1} FIP I sample. The flow rate is 1 ml h^{-1}.

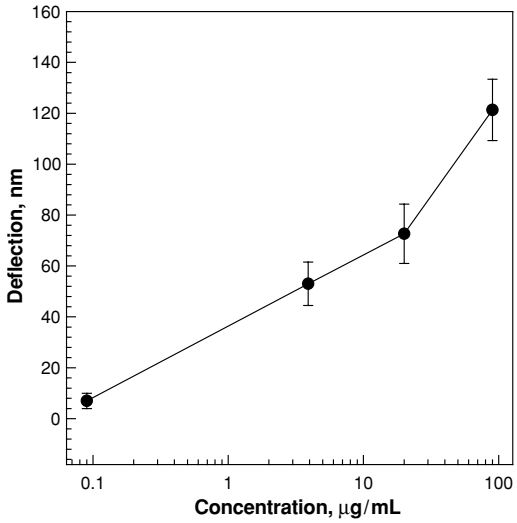

Figure 3. Deflection versus concentration of FIP antiserum modified microcantilevers. The flow rate is 1 ml h^{-1}.

Analytical procedure

The chemically modified microcantilevers were placed in the glass cell (figure 1, Digital Instruments, Santa Barbara, CA) whose volume is about 0.3 ml. The working solution, phosphate buffer solution, was run through the low pressure injection port sample loop system into the flow cell. Since a change in the flow rate would induce noise in the cantilever bending signal due to turbulence, the flow rate was maintained at a constant rate of 1 ml h^{-1} throughout the experiment. Analyte containing different concentrations of antigen dissolved in phosphate buffer solution was injected through the injection port sample loop system which allows for the continuous exposure of the cantilever to the desired solution. The bending of the cantilever was quantified using the instrument described above. The injection of the analyte was done after a stable baseline was obtained.

Three microcantilevers were prepared for each of the individual experiments allowing statistical comparison of repeatability and efficiency between devices and between techniques.

Results and discussions

Microcantilevers modified by both protocols responded to FIP I. However, the first protocol did not yield reproducible microcantilevers for FIP I detection. The deflection amplitudes were significantly different from cantilever to cantilever. It is known that surface modification plays a critical role in producing reproducible and reliable microcantilever sensors. FTIR, contact angle measurements showed that the surface modified by protocol one was not reproducible, to which we might attribute the poor quality of these cantilever sensors for FIP I detection.

The second protocol, on the other hand, provided a relatively reliable surface modification approach and the standard error was within 15%. All the results discussed in this paper were based on those cantilevers obtained from the second protocol.

Figure 2 shows a typical microcantilever deflection profile when a modified cantilever is exposed to a FIP I solution. FIP I was added at the marked time. A 2.0 ml aliquot of FIP I solution was switched into the fluid cell. It took approximately 2 h for the injected FIP I solution to flow through the fluid cell, and, immediately following the FIP I, water was circulated back through the fluid cell. First, the cantilever underwent an upward bending by a maximum of 50 nm in 1 h. When the FIP I was replaced by buffer, the cantilever bent backwards to its original position (i.e. zero deflection).

The control experiment performed with an antiserum conjugated microcantilever to a negative control sample that contains no FIP I antigen showed that no deflection of the cantilever was observed. Another control experiment was performed with an unmodified microcantilever to FIP I positive control and no deflection was observed upon exposure to the FIP I sample.

For a 50 nm deflection, the surface stress change was 0.11 N m^{-1} according to the following equation [27]:

$$\Delta Z = \left(\frac{3(1-\nu)L^2}{ET^2}\right)\delta s \qquad (1)$$

where ΔZ is the observed deflection at the end of the cantilever, ν and E are Poisson′s ratio (0.2152) and Young's modulus (155.8 GPa) for the silicon substrate, respectively, T is the thickness of the cantilever (1 μm), L is the length of the cantilever (180 μm) and δs is the differential stress on the cantilever.

Experiments performed under different flow rates showed that a lower flow rate gave larger bending amplitude. For instance, the maximum bending amplitudes at 2 ml h^{-1} and 8 ml h^{-1} upon exposure to 3.9 μg ml^{-1} of FIP I were 30 nm and 6 nm, respectively. The flow rate experiments indicated that the coronavirus particles take time to orient themselves in suitable positions atop the antibody molecules for binding and the binding was significantly affected by the environmental conditions, such as the flow rate. A reaction time of 45–60 min would be necessary in order to saturate the FIP antiserum–FIP

I binding under low flow rate conditions and it took a longer time to reach equilibrium under a higher flow rate.

It was also noted that the cantilever downward bending process was slower than upward bending, suggesting a slower unbinding process. It was anticipated that the Langmuir adsorption model could be used to describe the absorption of FIP I on the antibody covered surface. The rate of formation of a fraction of a monolayer, θ, is proportional to the concentration of the reacting species in solution and to the fraction of the surface remaining free of sorbant, $1 - \theta$. Thus, the cantilever bending versus the time follows the relationship [28]

$$\Delta Z = \left(\frac{3(1-\nu)L^2}{ET^2}\right)\delta s \propto 1 - \exp(-kt) \qquad (2)$$

where k is the reaction rate and t is the time.

k was calculated to be 0.05 s^{-1} using a nonlinear curve-fitting method to fit the observed experimental data. Similar treatment showed that the dissociation constant k' is 0.02 s^{-1}.

However, it should be noted that the fact that the response time of the sensor is not the same for binding and unbinding may also be due to the response of the fluid cell since the fluid cell we used was not a microfluid system [29]. Furthermore, recently investigations [30, 31] showed that the space arrangement for the cantilevers inside a fluidic cell, such as fluidic cell height and the distance between cantilevers and the wall of the fluidic cell, also play significant roles in sensing performance and microcantilever chip design. These may also affect the binding and unbinding rate calculations.

Figure 3 shows that the deflection amplitudes of the microcantilever were in proportion to the concentrations of FIP I injected. The standard error was within 15%. It shows that the microcantilever can be used for the detection of FIP I with a detection limit of 0.1 μg ml^{-1} when the assay time was <1 h. The detection limit was similar to that of ELISA in this relatively shorter detection time [32].

Summary

This work was aimed at validating the microcantilever sensor approach for the detection of feline coronavirus in solution. The sensor can detect a viral concentration as low as 0.1 μg ml^{-1}. A comparison of the detection limit with other methods cannot be made because no detection limit has been reported for FIP I detection by ELISA or PCR. It should by no means be concluded that this microsensor can be used to detect FIP I virus and SARS-CoV in a fast and single experiment at this moment, but these results demonstrated that coronavirus can be sensed by the deflection of microcantilevers and this work paves the way for the development of microcantilever sensors for human-associated SARS-CoV. Cross reactivity by using a microcantilever array modified by multiple antiserum or antibodies needs to be thoroughly investigated to conclude whether the microcantilever array can be used for fast and reliable SARS detection.

Acknowledgment

This work was partially supported by NSF Sensor and Sensor Network ECS-0428263.

References

[1] Anand K, Ziebuhr J, Wadhwani P, Mesters J R and Hilgenfeld R 2003 Coronavirus main proteinase (3CLpro) structure: basis for design of anti-SARS drugs *Science* **300** 1763–7

[2] Normile D and Enserink M 2003 Tracking the roots of a killer *Science* **301** 297–9

[3] Wu Q *et al* 2004 Development of Taqman RT-nested PCR system for clinical SARS-CoV detection *J. Virol. Methods* **119** 17–23

[4] Guan Y, Zheng B J, He Y Q, Liu X L, Zhuang Z X, Cheung C L, Luo S W, Li P H, Zhang L J and Guan Y J 2003 Isolation and characterization of viruses related to the SARS coronavirus from animals in Southern China *Science* **302** 276–8

[5] Holmes K V 2003 SARS coronavirus—a new challenge for detection and therapy *J. Clin. Invest.* **111** 1605–9

[6] Jiang S S, Chen T-C and Yang J Y 2004 Sensitive and quantitative detection of severe acute respiratory syndrome coronavirus infection by real-time nested polymerase chain reaction *Clin. Infect. Dis.* **38** 293–6

[7] Lau L T *et al* 2003 A real-time PCR for SARS–coronavirus incorporating target gene pre-amplification *Biochem. Biophys. Res. Commun.* **312** 1290–6

[8] Zuo B, Li S, Guo Z, Zhang J and Chen C 2004 Piezoelectric immunosensor for SARS-associated coronavirus in sputum *Anal. Chem.* **76** 3536–40

[9] Wu H-S, Hseih Y-C, Su I-J and Lin T-H 2004 Early detection of antibodies against various structural proteins of the SARS-associated coronavirus in SARS patients *J. Biomed. Sci.* **11** 117–26

[10] Zeng R, Ruan H Q and Ziang X S 2004 Proteomic analysis of SARS associated coronavirus using two-dimensional liquid chromatography mass spectrometry and one-dimensional sodium dodecyl sulfate-polyacrylamide gel electrophoresis followed by mass spectrometric analysis *J. Proteome Res.* **3** 549–55

[11] Chang M-S, Lu Y-T, Ho S-T and Wu C-C 2004 Antibody detection of SARS-CoV spike and nucleocapsid protein *Biochem. Biophys. Res. Commun.* **314** 931–6

[12] Gimzewski J K, Gerber C, Meyer E and Schlittler R R 1994 Observation of a chemical reaction using a micromechanical sensor *Chem. Phys. Lett.* **217** 589–94

[13] Chen G Y, Warmack R J, Thundat T, Allison D P and Huang A 1994 Resonance response of scanning force microscopy cantilevers *Rev. Sci. Instrum.* **65** 2532–7

[14] Thundat T, Warmack R J, Chen G Y and Allison D P 1994 Thermal and ambient-induced deflections of scanning force microscope cantilevers *Appl. Phys. Lett.* **64** 2894–6

[15] Fritz J M, Baller M K, Lang H P, Rothuizen H, Vettiger P, Meyer E, Guntherodt H-J, Gerber Ch and Gimzewski J K 2000 *Science* **288** 316

[16] Sepaniak M, Datskos P, Lavrik N V and Tipple C 2002 Microcantilever transducers: a new approach in sensor technology *Anal. Chem.* **74** 568A–75A

[17] Tang Y, Xu X, Fang J and Ji H-F 2004 Detection of femtomolar concentration of HF using an SiO_2 microcantilever *Anal. Chem.* **76** 2478–81

[18] Gotszalk T, Grabiec P and Rangelow I W 2000 Piezoresistive sensors for scanning probe microscopy *Ultramicroscopy* **82** 39–48

[19] Chu J, Itoh T, Lee C and Suga T 1997 Frequency modulation detection high vacuum scanning force microscope with a self-oscillating piezoelectric cantilever *J. Vac. Sci. Technol.* B **15** 1647–51

[20] Thundat T G and Wachter E A 1998 Microcantilever Sensor. *US Patent* #05719324 (Patent Feb. 17, 1998)

[21] Yan X, Zhang J, Ji H-F and Thundat T 2004 Biowarfare agents measurement using microcantilevers *Expert Rev. Mol. Diag.* **4** 859–66

[22] Addie D D and Jarrett J O 1992 A study of naturally occurring feline coronavirus infections in kittens *Vet. Rec.* **130** 133–7
[23] Hebben M, Duquesne V, Cronier J, Rossi B and Aubert A 2004 Modified vaccinia virus Ankara as a vaccine against feline coronavirus: immunogenicity and efficacy *J. Feline Med. Surg.* **6** 114–8
[24] Yan X, Tang Y, Ji H-F, Lvov Y and Thundat T 2004 Detection of organophosphate using an AChE-coated microcantilever *Instrum. Sci. Technol.* **32** 175–83
[25] Patel N, Davies M C, Hartshorne M, Heaton R J, Roberts C J, Tendler S J B and Williams P M 1997 Immobilization of protein molecules onto homogeneous and mixed carboxylate-terminated self-assembled monolayers *Langmuir* **13** 6485–90
[26] Ji H F, Thundat T, Dabestani R, Brown G M, Britt P F and Bonnesen P V 2001 Ultrasensitive detection of CrO_4(2-) using a microcantilever sensor *Anal. Chem.* **73** 1572–6
[27] Chen G Y, Thundat T, Wachter E A and Warmack R J 1995 Adsorption-induced surface stress and its effects on resonance frequency of microcantilevers *J. Appl. Phys.* **77** 3618–22
[28] Lang H P, Baller M K, Berger R, Gerber Ch, Gimzewski J K, Battiston F M, Fornaro P, Ramseyer J P, Meyer E and Guntherodt H J 1999 An artificial nose based on a micromechanical cantilever array *Anal. Chim. Acta* **393** 59–65
[29] Menil F, Susbielles M, Debeda H, Lucat C and Tardy P 2005 Evidence of a correlation between the non-linearity of chemical sensors and the asymmetry of their response and recovery curves *Sensors Actuators* B **106** 407–23
[30] Khanafer K, Khaled A-R A and Vafai K 2004 Optimization modeling of analyte adhesion over an inclined microcantilever-based biosensor *J. Micromech. Microeng.* **14** 1220–9
[31] Khaled A-R A and Vafai K 2004 Spatial optimization of an array of aligned microcantilever biosensors *J. Micromech. Microeng.* **14** 1328–36
[32] Teramoto Y A, Mildbrand M M, Carlson J, Collins J K and Winston S 1984 Comparison of enzyme-linked immunosorbent assay, DNA hybridization, hemagglutination, and electron microscopy for detection of canine parvovirus infections *J. Clin. Microbiol.* 373–8